COO-2853-10
CONF-800131--3

Invited paper presented at the Los Alamos Scientific Laboratory on "Nuclear Structure Physics with Intermediate Energy Probes," January 14-16, 1980, Los Alamos, New Mexico.

180° ELECTRON SCATTERING

MASTER

by

G.A. Peterson
Department of Physics and Astronomy
University of Massachusetts
Amherst, Massachusetts 01003

ABSTRACT

Electron scattering transverse form factors are sensitive to nuclear dynamical properties such as convection, spin, and exchange currents. They provide sensitive tests of nuclear wave functions and can be readily compared to data obtained by using other probes. Recent measurements of transverse form factors by 180° electron scattering are described.

I. INTRODUCTION

High momentum transfer elastic and inelastic electron scattering at forward angles has provided excellent descriptions of nuclear ground state charge distributions and of transition charge densities. From such measurements detailed pictures of the sizes and shapes of nuclei can be deduced. On the other hand, electron scattering at backward angles is sensitive to the magnetic properties of nuclei. In the nuclear ground state these properties are generally determined by a few unpaired valence nucleons which contribute to the magnetization through their intrinsic spin currents, and in the case of protons, through their orbital currents. Similarly inelastic exci ations may involve spin magnetization and convection current densities. By observing electrons scattered through 180°, such magnetic cross sections may be measured in the relative absence of charge cross sections. A system of magnets[1] for 180° electron scattering measurements has been constructed by the University of Massachusetts for use at the Bates Linear Accelerator. The features of this system, the interpretation of recent measurements, and possible future studies will be discussed.

DISCLAIMER

II. APPARATUS

A system of four dipole magnets was built to operate in an energy-loss mode in conjunction with the high-resolution 90° spectrometer[2] for electrons having energies up to 450 MeV. The principle of operation may be understood from Fig. 1. The beam travels through equal path lengths in each of the three magnets D1, D2, and D3 of equal field strengths B, which serve only as beam transport elements. The fourth magnet bends the beam along its initial direction before it strikes the target. The back-scattered electrons are then deflected through an angle α_o and go into the spectrometer. The forward-going electrons, which have undergone small-angle multiple scattering in the target, travel about 20 meters downstream before they are deflected by a pair of large iron-free coils so as to prevent back-scattering from the beam catcher. In order to observe inelastically scattered electrons, the fields in all of the magnets are reduced, and the center magnets D2 and D3 are moved closer to the incident beam line, thereby reducing the angle α of Fig. 1. The angle α_o to the spectrometer however remains fixed. Thus a constant solid angle for 180° scattering is maintained, regardless of inelasticity. A side view of this assembled system is shown in Fig. 2. In order to convert back to forward-angle scattering conditions, it is only necessary to remove D4, and to insert the usual scattering chamber at the spectrometer's center of rotation. The 180° scattering apparatus has been used routinely for the past two years. Resolutions of less than 2.5×10^{-4} and cross sections of less than 10^{-36} cm^2/sr have been measured.

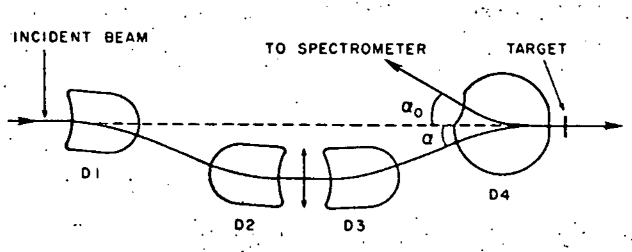

Fig. 1.
Schematic diagram of four dipole magnet system for 180" electron scattering.

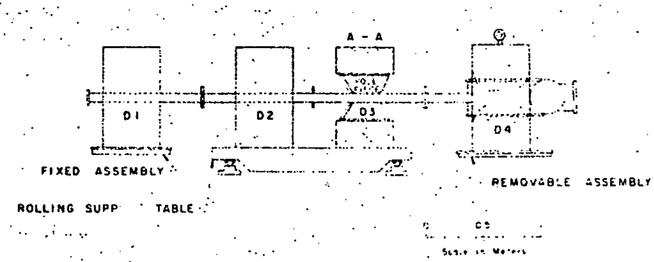

Fig. 2.
Side view of apparatus. The middle two magnets move in a horizontal plane perpendicular to the beam line.

III. FORMALISM

In the plane-wave one-virtual photon exchange approximation the differential cross section for an electron of energy E_o to scatter through an angle θ when interacting with a nucleus of charge Ze is given by[3]

$$\frac{d\sigma}{d\Omega} = \frac{4\pi\sigma_M}{\eta} \left[|F_L(q)|^2 + \left(\frac{1}{2} + \tan^2 \frac{\theta}{2}\right) |F_T(q)|^2 \right]. \qquad (1)$$

Here η is a recoil factor, and

$$\sigma_M = (Z\alpha/2E_o)^2 (\cos^2 \frac{\theta}{2} / \sin^4 \frac{\theta}{2}) \qquad (2)$$

is the point Mott cross section. The longitudinal and transverse form factors $F_L(q)$ and $F_T(q)$ are functions of the momentum transfer q and contain the nuclear structure information. The longitudinal form factor is given by

$$F_L(q) = \frac{\sqrt{2\lambda + 1}}{Z} \int_0^\infty j_\lambda(qr)\ Y_{\lambda M}(\Omega) \rho_{fi}(\vec{r}) dr^3, \qquad (3)$$

where $\rho_{fi}(\vec{r})$ is the transition charge density operator and λ is the transition multipolarity. The transverse form factor is given by

$$F_T(q) = [Z(2J_i + 1)]^{-1} [T_j(q) + T_m(q)], \qquad (4)$$

where the amplitude T_j contains the convection current operator $e\vec{j}(\vec{r})$ and the amplitude T_m contains the spin magnetization density operator $e\vec{\mu}(\vec{r})$.

By examining Eqs. (1) and (2) it can be seen that in this approximation the longitudinal cross sections vanish at 180°, and that $|F_T(q)|^2$ can therefore be measured by itself. An expansion of Eq. (1) about $\phi = 180° - \theta$ shows a parabolic dependence of the cross sections on ϕ. Figure 3 shows this dependence for scattering from the ^{12}C $J_i = 0$ ground state, where the finite solid angle includes some charge scattering at $\theta < 180°$. Such scattering from charges is usually small enough to be of little consequence for electron energies larger than 100 MeV.

IV. ELASTIC MAGNETIC SCATTERING

For nuclei with $J_i \geq 1/2$, 180° elastic scattering can take place from the magnetic multipole moment distributions. It is limited to the odd magnetic multipoles by time reversal and parity considerations. As an example,[4-6] Fig. 4 shows the form factor of ^{93}Nb. Since $J_i = 9/2$, all odd-magnetic multipoles up to M9 contribute. Other experimental techniques, such as NRM or electronic hyperfine shifts give information only on the M1 and M3 moments at the q = 0 limit.

Magnetic elastic scattering gives information on the radial distribution of the nuclear magnetization and hence of the valence nucleons. Another way of getting valence nucleon radial information is by finding the difference between the charge distributions of isotone pairs, wherein the charge distribution of the odd-proton plus its core polarization is mapped out.[7] An experiment[8] will get underway this spring at Bates to make a direct comparison of isotone difference charge scattering and magnetic scattering from ^{29}Si, ^{30}Si, and ^{31}P. A comparison of these results should be consistent, but if it is not, perhaps some

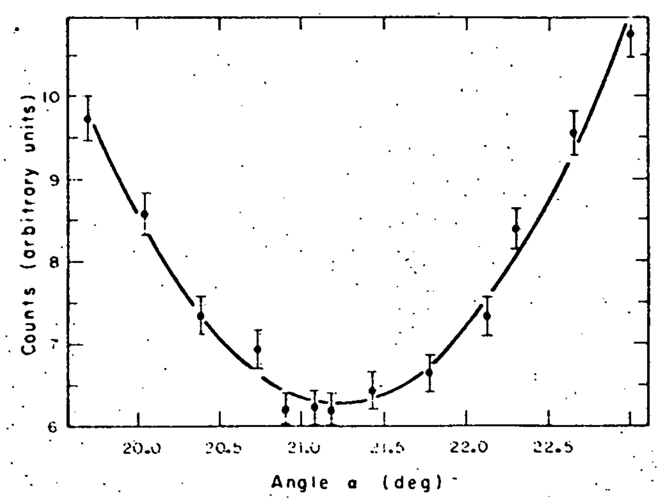

Fig. 3.
Counts versus D4 entrance angle α for the elastic scattering of 57 MeV electrons from ^{12}C. The 180° scattering angle corresponds to α = 21.3°.

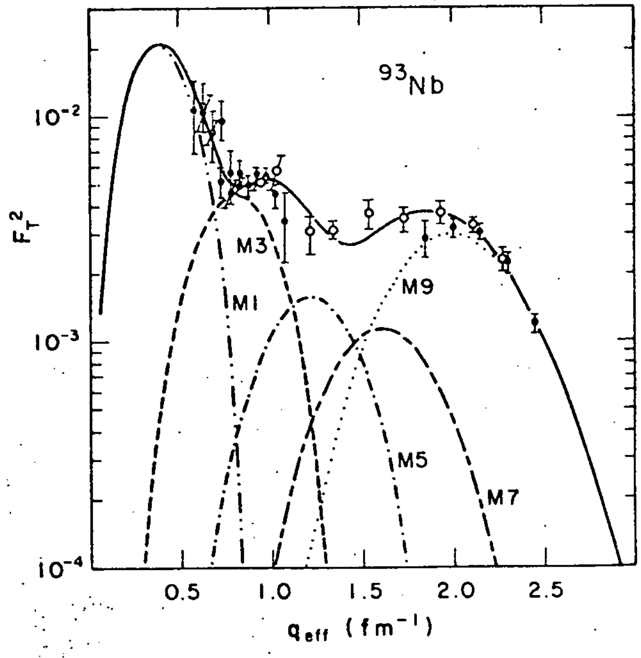

Fig. 4.
Elastic magnetic form factor of ^{93}Nb. The open circles are 180° Bates data,[4] the low q closed circles 180° Amsterdam data, and the high q closed circles Saclay data.[5]

new physics can be learned. The distribution of the valence neutron and proton will be mapped out for ^{29}Si and ^{31}P, respectively.

Figure 5 shows preliminary results for the M1 form factor of ^{13}C. Since only the magnetic dipole moment distribution is involved, the interpretation should be especially clean, and will not involve confusion with respect to the contributions of the higher multipoles. It is expected that the large form factor at high momentum transfer may have large exchange current contributions.

The scattering of hadronic probes has also been used in studying the radial extension of valence nucleons, for example, by pick-up reactions. But the interpretation of such results involves the uncertainties of the strong interaction.[10] Furthermore, the anomalous hyperfine splitting of levels in muonic atoms can yield radial information, but this technique is limited to high-Z nuclei.

V. CONVECTION-, SPIN-, AND EXCHANGE-CURRENTS, AND OTHER EFFECTS

The amplitudes T_j and T_m can give rise to sensitive cancellations in the transverse form factor. An example is shown in Fig. 6 for the ^{12}C 9.6 MeV collective 3^- excitation.[11] Here a simple $d_{5/2}p_{3/2}^{-1}$ configuration is used in calculating the transverse electric form factor. The convection current part taken by itself is shown by the dashed lines, and the magnetization current part by itself by the dashed-dotted line. However, the convection current and magnetization amplitudes have opposite signs in the momentum transfer region where our measurements were made. Consequently the form factor which is proportional to the sum of these amplitudes, has a minimum at about $q = 1.5\ fm^{-1}$. Its square is shown by the solid line in Fig. 6. On the other hand, an SU-3 calculation by Millener[12] gives a large convection current part compared to a weak magnetization part[11] as shown in Fig. 7. This calculation, which perhaps indicates the alpha cluster-like nature of ^{12}C, clearly gives the correct shape to the form factor. Incidentally, this normal parity transition has a large longitudinal form factor, and a weak transverse electric form factor. It is unlikely that this transverse form factor could be measured at any other angle than 180° where longitudinal parts are suppressed. The measurement of the convection current part of the 4.44 MeV collective 2^+ transition in ^{12}C has also been reported in a recent communication.[13] In contrast to the sensitivity of the cancellations of T_j and T_m in producing a minimum in $|F_T|^2$, the spherical

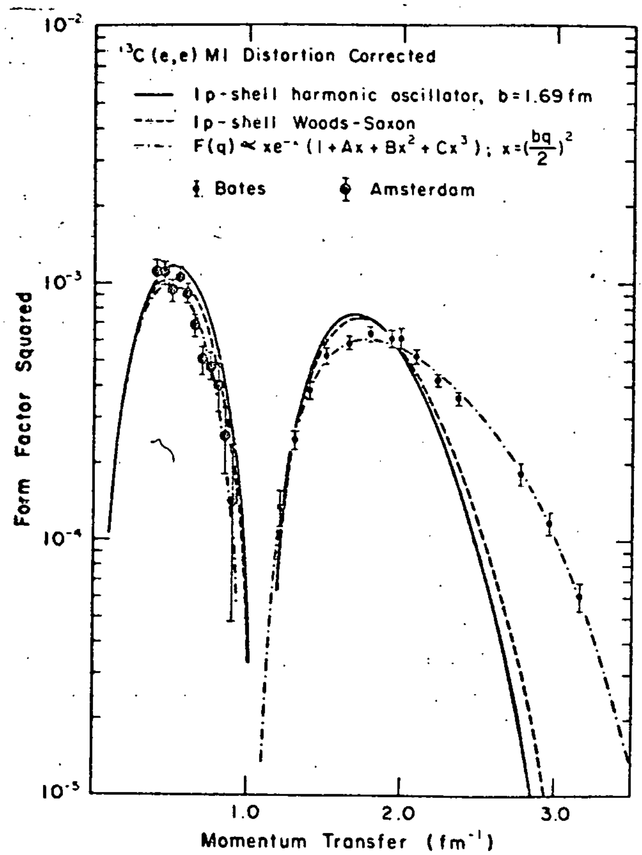

Fig. 5.
The square of the distortion corrected elastic M1 form factor for ^{13}C.

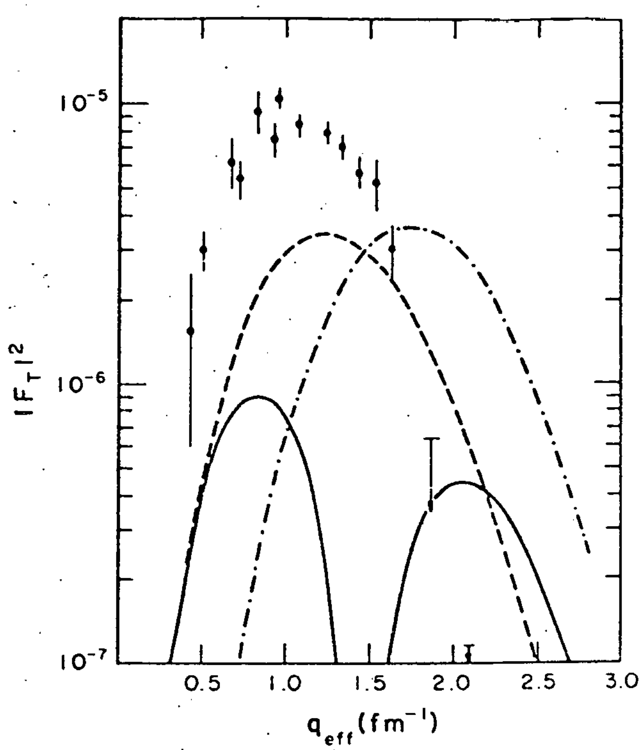

Fig. 6.
$|F_T|^2$ for ^{12}C 9.6 MeV 3^- state calculated with $d_{5/2}p_{3/2}^{-1}$ configuration as explained in text.

Bessel function $j_\lambda(qr)$ may determine the minimum in $|F_L|^2$, as can be seen from Eq. (3).

In the amplitude $T_m(q)$ the magnetic moment operator for an isoscalar transition involves $\mu_p + \mu_n$, and that of an isovector transition $\mu_p - \mu_n$. Thus the ratio of the cross section of an isoscalar transition to that of an isovector transition is proportional to $[(\mu_p + \mu_n)/(\mu_p - \mu_n)]^2 = 1/28.6$. Furthermore, the dominant exchange current effects will appear in the isovector and not the isoscalar transition. The exchange currents form factors are expected to have a q dependence such that the maximum is reached at about twice the corresponding q of the one-body interaction part of the form factor.[14] For example, electron scattering from the deuteron[15] shows a small elastic T=0 cross section at 180° proportional to $(\mu_p + \mu_n)^2$, whereas the M1 spin-flip T=1 section is proportional to $(\mu_p - \mu_n)^2$. The latter is quite large and has very large exchange currents.

Other comparisons between T=0 ground states and T=1 excited states are possible for odd Z-odd N nuclei. Measurements are generally lacking for most of these nuclei, but preliminary evidence from a Bates Linac experiment by Bergstrom et al.[16] shows that the ^{6}Li T=0 elastic 1^{+} M1 form factor falls off at high q, but that the M1 form factor for the transition to the T=1 3.56 MeV 0^{+} state remains large, thus perhaps indicating the strong presence of isovector exchange currents in the excited state. These data cannot be explained by nuclear structure differences between the two states, since presumably very similar p-shell radial wave functions are involved.

Another comparison between T=0 and T=1 states has been made for the M1 transitions in ^{12}C to the 12.71 and 15.11 MeV 1^{+} states. The form factor data for the latter transition are shown in Fig. 8. Dubach and Haxton[17] have considered the role of exchange currents in these excitations. Although high-q electron scattering data can provide constraints on nuclear structure analyses, Dubach and Haxton point out that the usefulness of the data is seriously impaired

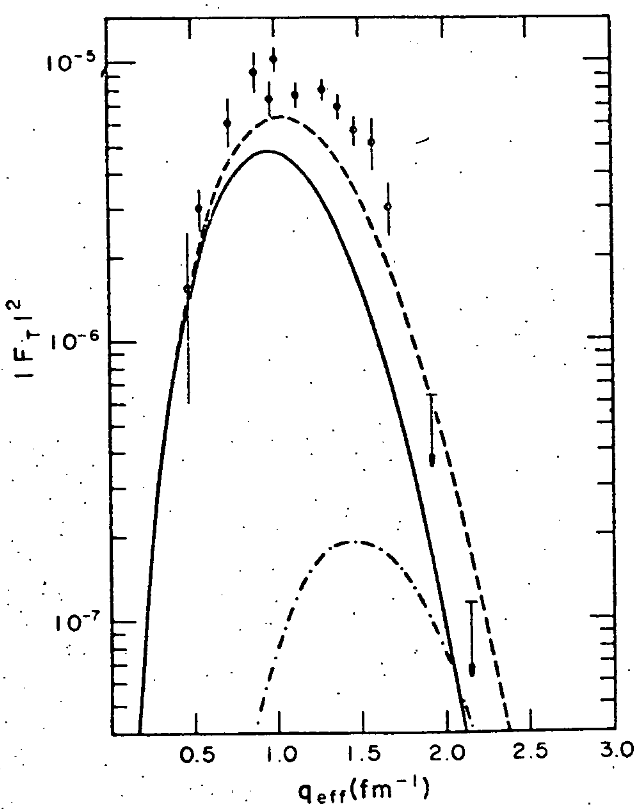

Fig. 7.
^{12}C 9.64 MeV 3^{-} form factor. Curves were calculated in an SU-3 basis.

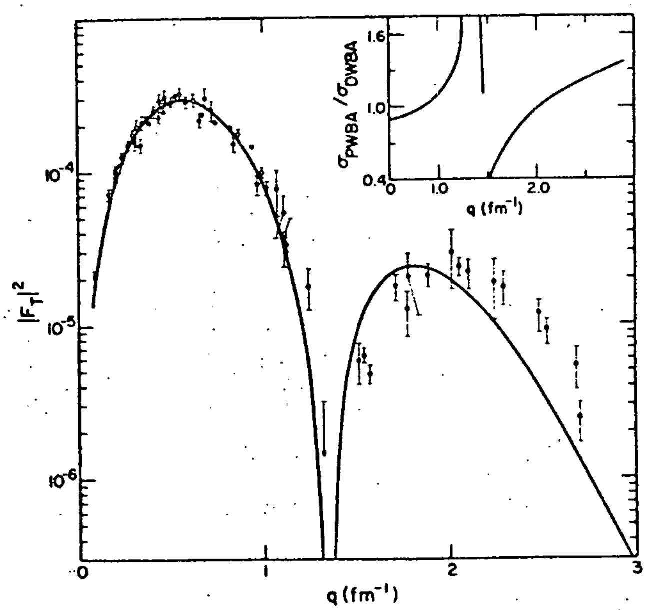

Fig. 8.
^{12}C 15.11 MeV 1^{+} form factor. Calculated curve includes exchange currents.

if meson-exchange currents are not included in calculations of (e,e') form factors. In lowest order, exchange current effects are expected to have no effect on the isoscalar transition to the 12.71 MeV state.

The 15.11 MeV form factor also seems to have no bottom in its measured minimum. This lends support to the assumption of single virtual photon exchange, and the lack of virtual excitation and deexcitation by so-called dispersion scattering.[2] Also note that the high q data are above the calculated curve. Attempts have been made to explain this discrepancy by evoking pion condensation,[18] and by considering the ρ meson in the polarizing interaction. Nevertheless, a Migdal parameter g' = 0.39 was required to give a reasonable fit to the data. This is smaller than the usual accepted values.

Figure 9 shows the form factor of the much weaker (~ 1/100) 12.71 MeV T=0 transition. It is strikingly different from the 15.11 MeV T=1 form factor. The upper curves of Fig. 9 indicate isospin mixing[19] from the T=1 level. The solid curve and the dashed curve were calculated using a different combination of potentials. It is clear that at low q there is little sensitivity to the potential, but a large sensitivity to the degree of isospin mixing. From these results, a charge-dependent isospin-mixing matrix element ranging from 130 to 165 keV was deduced, which might be atrributed to a charge-dependent component in the strong interaction.[19]

The 12.71 MeV T=0 state also may be of importance in learning about axial isoscalar neutral currents. A predicted asymmetry[20] for polarized (e,e') scattering is at a maximum at 180° as shown in Fig. 10. Present experiments yield information on the isovector component.

As was mentioned before, meson exchange currents produce large effects in the transverse cross section of deuteron electrodisintegration near threshold. This is shown in Fig. 11, part of a contour plot of Fabian and Arenhovel.[21] However, Fig. 11 shows that at high excitation energies, $|F_T|^2$ can increase by over 50% because of virtual isobar configuration excitations. Work is in progress to look for these effects at 180° where there is a maximum sensitivity.

Figure 12 shows a spectrum for ^{208}Pb. The $|F_T|^2$ for the 7.45 MeV peak has an M1-like shape.

We have shown that the electron is a spin-sensitive and current-sensitive probe when used in 180° scattering experiments. Since the large Coulomb contributions are suppressed, it permits the observation of delicate nuclear structure effects.

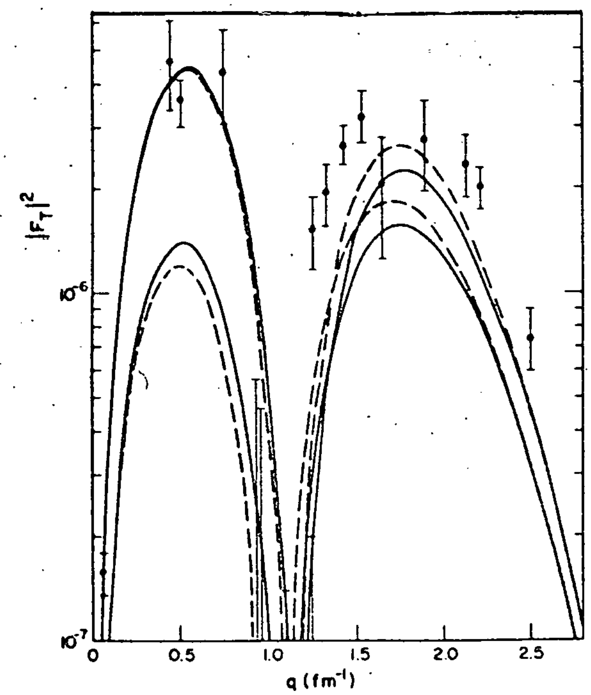

Fig. 9.
^{12}C 12.71 MeV 1^+ form factor.

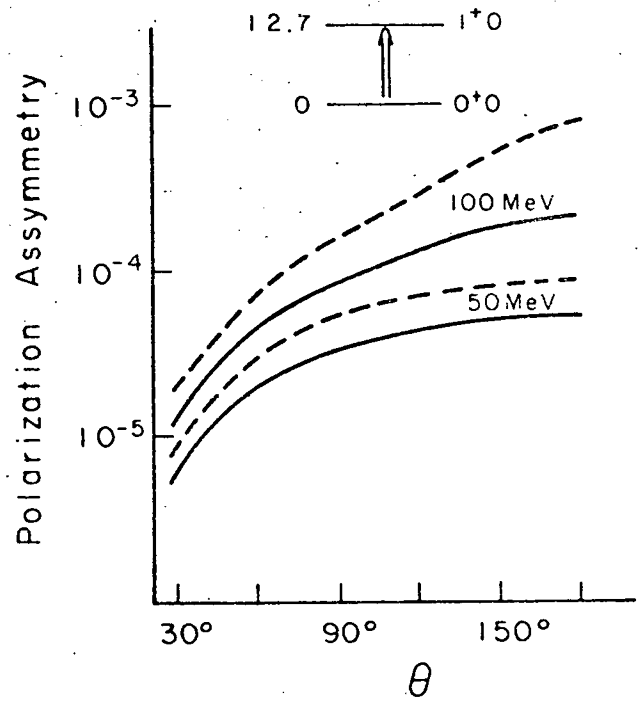

Fig. 10.
^{12}C 12.71 MeV $(\vec{e},\vec{e}')$ asymmetry.

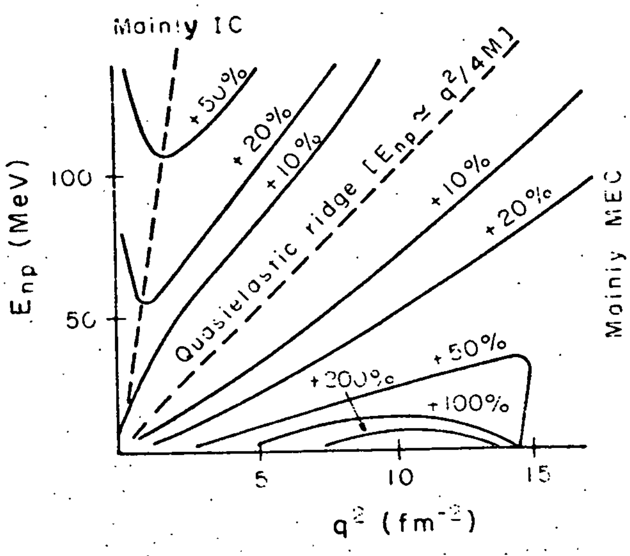

Fig. 11.
Percent change in $|F_T|^2$ of d(e,e') for exchange current and isobar effects.

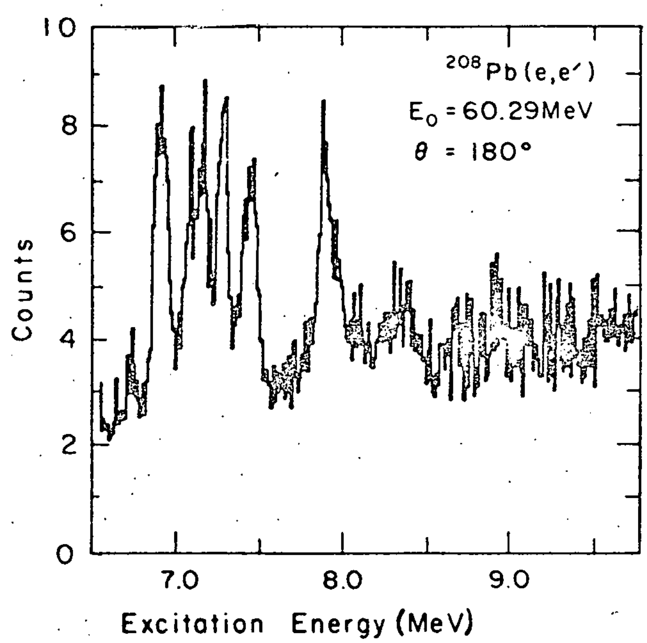

Fig. 12.
Portion of 180° (e,e') spectrum.

ACKNOWLEDGMENTS

Many discussions with J. Flanz, R. Hicks, and R. Lindgren are gratefully acknowledged. Mrs. Doris Atkins deserves thanks for her patience in the last-minute preparation of this report. This work was supported in part by funds provided by the U.S. Department of Energy and the University of Massachusetts.

REFERENCES

1. G.A. Peterson et al., Nucl. Instr. and Meth. 160, 375 (1979).

2. W. Bertozzi et al., Nucl. Instr. and Meth. 162, 211 (1979).

3. T. deForest, Jr. and J.D. Walecka, Adv. Phys. 15, 1 (1966).

4. R.C. York and G.A. Peterson, Phys. Rev. C19, 574 (1979).

5. G. Box, Ph.D. Thesis, I.K.O., Amsterdam, 1976 (unpublished).

6. P.K.A. deWitt Huberts et al., Phys. Lett. 60B, 157 (1976).

7. B. Sinha et al., Phys. Rev. C6, 1657 (1972).

8. H. Miessen et al., Bates Proposal #7814, March, 1979 (unpublished).

9. R. Hicks et al., Bates Proposal #782, March, 1978 (unpublished).

10. L. Lapikas, Proc. of Mainz Conference, Lecture Notes in Physics, Vol. 108, (Springer-Verlag, New York, 1979), pp. 41-51.

11. J.B. Flanz, thesis, U. of Mass., 1979 (unpublished).

12. D.J. Millener, private communications.

13. J.B. Flanz et al., Phys. Rev. Letters 41, 1642 (1978).

14. T.W. Donnelly, private communications.

15. G.A. Peterson and W.C. Barber, Phys. Rev. 128, 812 (1962).

16. J.C. Bergstrom, private communications.

17. J. Dubach and W. Haxton, Phys. Rev. Letters 4 , 1453 (1978).

18. J. Delorme, M. Ericson et al., Univ. C.B. Lyo -1, Villeurbanne Cedex, France (preprints).

19. J.B. Flanz et al., Phys. Rev. Letters 43, 1922 (1979).

20. J. Bernabéu and R.A. Eramzhyan, Phys. Letters 80B, 396 (1979).

21. W. Fabian and H. Arenhövel, Nucl. Phys. A314, 253 (1979).